Research Article

Solution Uptake in Cylindrical Carbon-Fibre-Reinforced Polymer (CFRP) Tendons

Paul Scott,[1] Eleni Toumpanaki,[2] and Janet M. Lees[3]

[1]*Cambridge Design Partnership, Church Road, Toft, Cambridge CB23 2RF, UK*
[2]*University of Bristol, Department of Civil Engineering, University Walk, Bristol BS8 1TR, UK*
[3]*Department of Engineering, Civil Engineering Building, University of Cambridge, JJ Thomson Ave 7a, Cambridge CB3 0FA, UK*

Correspondence should be addressed to Eleni Toumpanaki; eleni.toumpanaki@bristol.ac.uk

Received 15 June 2022; Revised 20 October 2022; Accepted 29 October 2022; Published 30 November 2022

Academic Editor: Wen Li

Salt water exposure conditions relevant to carbon-fibre-reinforced polymer (CFRP) prestressed concrete structures in marine environments are investigated. The diffusion into relatively small diameter CFRP tendons can be a lengthy process so the prediction of the long-term moisture uptake using short-term experiments on thin films of epoxy would be advantageous. However, the fibre inclusions within a composite introduce complexities, and factors are typically required for correlation with pure epoxy specimens. Diffusion parameters based on moisture uptake result from CFRP tendons exposed to salt water solution at 20°C and 60°C are compared with those obtained using equivalent thin film specimens. The higher temperature is selected to accelerate the moisture uptake. It is found that the measured ratios of tendon and epoxy diffusivity were temperature dependent, and the combination of the higher temperature and salt solution leads to an increased propensity for moisture uptake in the tendon. Existing analytical models to predict the CFRP tendon diffusivity from that of a thin film of epoxy did not appear to capture the observed trends. However, predictions using a unit cell with a fibre interface zone suggest that this may be due to an increased diffusivity in the interphase region.

1. Introduction

The durability of fibre-reinforced polymers (FRPs) is often cited as one of the key drivers for the use of FRP materials in demanding civil engineering applications. Unlike steel, FRPs do not corrode. However, FRPs can be susceptible to other mechanisms that can change their mechanical properties over time. As many civil engineering structures will be in service for decades, or even centuries, it is important to assess the potential implications of any changes in material properties on the long-term structural performance.

For FRP-prestressed concrete applications, the FRP tendon requirements include a high strength and stiffness and a good bond with the surrounding concrete. Unidirectional carbon-fibre-reinforced polymer (CFRP) pultrusions with a high fibre-volume fraction are therefore well-suited for use as prestress tendons. Tendons with a cylindrical cross-section are also common. When assessing the long-term durability, the structural response when subjected to aggressive exposure conditions is important and, for marine applications, this includes an understanding of how salt water solution moves in to carbon/epoxy tendons.

There are many variables in CFRP composites including the void content in the fibres and epoxy, the fibre diameter, the properties of the interphase region, and differences in manufacturing (e.g., curing conditions). A further consideration with cylindrical CFRP tendons is that the diffusion is three-dimensional. To fully reflect all of these variables, tests on the moisture uptake in the actual tendon are desirable. But as the diameter of CFRP tendons can be relatively large, say 4-16 mm, the time to conduct such tests can be prohibitive. Elevated temperatures will accelerate the uptake time but may influence the diffusion mechanisms. Since carbon fibres are typically considered to be impermeable, the diffusion parameters of the matrix (e.g., D_e) determined from short-term moisture uptake tests on thin epoxy-only films have been used to predict the corresponding parameters for a CFRP tendon (e.g., for the diffusion parallel, D_{11}, or

transverse to the fibre direction, D_{22}). However, to do this, adjustments are required to reflect the presence of the carbon fibres and various "knockdown" approaches/factors have been proposed in the literature.

The difficulties associated with relating the diffusion in an epoxy film to that of a corresponding CFRP tendon will be explored in the current work. Existing analytical models for the prediction of D_{22}/D_e "knockdown" factors are reviewed and benchmarked against experimental findings available in the literature. Mass uptake experiments on epoxy thin films and CFRP tendons with a comparable epoxy matrix subjected to salt water solution at 20°C or 60°C are reported. The resulting diffusion coefficients of the films and tendons enable the calculation of experimentally derived "knockdown" factors that can be used to assess the validity of analytical predictions for the diffusion of CFRP cylindrical specimens based on thin film results. The important question of whether the nature of uptake in the composite differs from that of the matrix is discussed. In particular, the possible effect of higher diffusivity in fibre-matrix interphase areas on the transverse diffusivity of CFRP tendons is considered.

2. CFRP Material Properties and Moisture Uptake

The structure of carbon fibres is widely reported as turbostatic [1]. Although surface pores of 4–6 nm diameters have been observed [2] and pores of around 16 to 18% of the fibre volume may exist within carbon fibres [3], for the most part the pore structure is reported as being closed [4]. As such, the uptake into carbon fibres is generally considered to be negligible in comparison with that of the surrounding polymer matrix [5–10], and so for the purposes of this investigation, the carbon fibres will be considered as impermeable.

An epoxy matrix is a thermoset polymer formed by curing an epoxy polymer with a hardener to form a crosslinked finished product [11]. Aqueous solution uptake occurs due to the permeability of the epoxy [12], the occupation of the free volume that is inherently dependent on the cross-linking density and an affinity between the hydroxyl (OH) polar groups in the epoxy and the polar water molecules [13]. The bound water molecules result in the swelling and plasticisation of the epoxy matrix. A second category of bound water molecules that cause secondary cross-linking via a higher degree of hydrogen bonding has been reported and is more likely to form at high temperature and longer exposure times due to the higher activation energy required [14]. Other secondary factors that can affect moisture diffusion in epoxies are the development of a two-phase structure due to incomplete curing [15] or stoichiometric composition [16] and the polymer polarity (electrostatic attraction between water and the polymer network) [15].

The moisture absorption of a CFRP profile will differ from that of a geometrically equivalent resin profile. The impermeable carbon fibres act as both an inhibitor of moisture absorption, reducing the solution uptake at saturation, and as a barrier to diffusion thereby affecting the diffusivity of the composite. The extent to which these phenomena occur depends primarily on the volume fraction. Voids and defects can also play a major role on the absorption process. Uptake through defects occurs by capillary flow, and it has been reported that such uptake may exceed uptake due to diffusion through the matrix [6]. However, the effect is mitigated through good quality control associated with the pultrusion manufacturing process [17]. Several US manufacturers contacted by Sen et al. [18] indicated that a 2% void content could be expected in CFRP pultruded tendons.

Studies have also shown that in close proximity to fibres, in the fibre-matrix interface region, diffusion may occur differently to that observed in the matrix. It has been argued that the diffusivity in this region is greater than that of the matrix [7, 10]. This can be attributed either to voids or the development of a softer interphase region due to incomplete curing [19] or different stoichiometric composition due to the reactivity between the fibre sizing and the bulk matrix [20, 21]. Experiments by Adams and Singh [22] where CFRP specimens were subjected to steam at 100°C found the observed solution uptake to be 27% higher than could be explained by the uptake observed in the epoxy matrix. However, the aggressive exposure conditions may have led to damage such as fibre/matrix delamination or matrix cracking. Ramirez et al. [23] showed that the moisture accumulation in the fibre/matrix interface is higher in carbon/vinyl ester than in carbon/epoxy composites. In the latter case, 50% of the solution uptake at saturation was attributed to fibre/matrix interfacial bond degradation after exposure in water. The importance of fibre/matrix interfacial properties has also been highlighted in Wang et al. [24] where composites with untreated carbon fibres exhibited approximately 1.9 and 2.6 times higher solution uptake at saturation than epoxy and composites with treated carbon fibres, respectively. Interphase regions with a thickness of 0.4-1.0 μm [25] and fibre/matrix debonding and microcracking [26] have been reported based on microscopic studies on CFRP/vinyl ester rods and CFRP/epoxy strips, respectively, after immersion in water. However, even in cases where no damage or degradation was reported, levels of solution uptake at saturation in composite specimens that are up to 66% higher than theoretical calculations have been observed [10]. These findings suggest that the presence of fibres in an epoxy increases the amount of solution that can be absorbed in the surrounding epoxy. Any concurrent degradation of this interphase during hygrothermal exposure would further hinder an in-depth understanding of the diffusion kinetics and need to be reflected in analytical models.

3. Diffusion Modelling

Composite tendons used in civil engineering applications generally represent fairly thick sections and take a relatively long time to saturate. So, a common approach to infer the composite behaviour is to consider the matrix as an isotropic material for diffusion purposes and apply factors to the matrix diffusion properties and the predicted mass at saturation to account for the presence of fibres. In the following, both Fickian and non-Fickian or anomalous diffusion

models will be discussed initially in the context of isotropic thin film and cylindrical geometries. Consideration is then given to direction-dependent diffusion in fibre-matrix composites.

3.1. Direction-Independent Fickian Diffusion. Fickian diffusion is based on Fick's first and second laws. Further details of the derivations that follow can be found in Crank [27]. One-dimensional Fickian diffusion is widely used to model the solution uptake in thin films [28]. Fick's second law can also be applied to a cylindrical tendon of radius, a, considering purely radial diffusion and a submerged boundary condition. When the outermost surface is saturated having a concentration C_0, the solution concentration in the initially dry cylinder at any radial position, r, and time, t, can be evaluated using

$$C(r,t) = C_o - \frac{2C_o}{\alpha}\sum_{n=1}^{\infty}\frac{\exp\left(-D\alpha_n^2 t\right)J_o(r\alpha_n)}{\alpha_n J_1(\alpha\alpha_n)}, \quad (1)$$

where D is the diffusion coefficient, and the α_n terms are the n^{th} positive roots of the Bessel function of the first kind of order zero, J_0. J_1 is the Bessel function of the first kind of the first order. Exact expressions exist to allow calculation of the percentage mass increase through integration of the concentration gradient in a submerged, initially dry cylinder to give

$$\frac{M_t}{M_\infty} = 1 - \frac{4}{\alpha^2}\sum_{n=1}^{\infty}\frac{\exp\left(-D\alpha_n^2 t\right)}{\alpha_n^2}, \quad (2)$$

where M_t is the mass at time t, and M_∞ is the mass at saturation.

3.2. Direction-Independent Anomalous Diffusion. A number of models have been proposed to reflect non-Fickian or anomalous diffusion behaviour and have been summarised in publications elsewhere, e.g. [28, 29],. Of particular interest in the current work is the relaxation-dependent Langmuir model [10, 13, 27, 29, 30]. Relaxation-dependent models assume that on initial exposure to moisture, an epoxy has a given capacity for absorption. As time progresses, the chemical interactions between the diffusing substance and the epoxy cause the material to swell, resulting in additional capacity for moisture absorption. A one-dimensional formulation of the Langmuir model was used to predict the anomalous behaviour of the epoxy films and tendons studied in the current work. However, the one-dimensional formulation could not readily be extended to give closed-form three-dimensional expressions. So, instead, a finite difference approach was used for the Langmuir prediction of the diffusion through a cylindrical tendon. For further details, please see [31].

3.3. Direction-Dependent Diffusion in Fibre-Matrix Composites. In the approaches described in the previous sections, the material is assumed to be isotropic. Epoxy thin film experiments enable the calculation of the diffusivity of the solution through the pure matrix, D_e, and the mass uptake at saturation $M_{\infty,e}$. The challenge is to then determine the analogous parameters for a fibre-reinforced system; namely, the mass uptake at saturation in the composite $M_{\infty,c}$ and the diffusivity of a solution parallel to the fibre direction, $D_{11,c}$, and transverse to the fibre direction, $D_{22,c}$.

3.3.1. Mass Uptake at Saturation $M_{\infty,c}$. The solution concentration at saturation in a composite, $C_{0,c}$, can be determined using the rule of mixtures [32]

$$C_{0,c} = \left(1 - V_f\right)C_{0,e}, \quad (3)$$

where $C_{0,e}$ is the solution concentration at saturation in the epoxy, and V_f is the fibre-volume fraction. This relationship assumes an absence of voids and sound fibre-matrix bonding, and that the fibre-matrix interface does not chemically alter the diffusion process. The $M_{\infty,c}$ in a unit volume of CFRP material can then be calculated as

$$M_{\infty,c} = 100\frac{M_{\text{eff}}C_{0,c}}{\left[\rho_r\left(1 - V_f\right) + \rho_f V_f\right]}, \quad (4)$$

where M_{eff} is the mass of one mole of molecules and ρ_r and ρ_f are the resin and fibre density, respectively.

3.3.2. Diffusion Parallel to the Fibre Direction-$D_{11,c}$. Kondo and Taki [32] argue that the diffusion coefficient parallel to the fibre direction $D_{11,c}$ should take the same value as that of the matrix, D_e, given that the fibres do not obstruct the flow of solution. However, others [8, 9, 33] suggest $D_{11,c}$ should take into account the presence of impermeable fibres, where

$$D_{11,c} = \left(1 - V_f\right)D_e. \quad (5)$$

As the total flux of solution transmitted is inversely proportional to the fibre-volume fraction, it follows that the diffusion coefficient could be expected to follow a similar relationship. Equation (5) relies on the assumption of a perfect fibre/matrix interfacial bond and absence of interphase region. This equation has been used in the current work.

3.3.3. Diffusion Transverse to the Fibre Direction-$D_{22,c}$. The evaluation of the transverse diffusivity, $D_{22,c}$, is complex and has received more consideration in the literature. Efforts have been made to assess the effect of fibre-volume fraction on transverse diffusivity using analogies with heat transfer, electrical conduction, or numerical simulations of solution flux [10]. These include the numerical method proposed by Keller and Sachs [34] and two models based on heat transfer analogies, the series-parallel (SP) approximation and the parallel-series (PS) approximation, described by Ko [35] to relate diffusivity in an epoxy to transverse diffusivity in a composite. Finite element predictions by Kondo and Taki [32] and Bond [10] of transverse diffusivity through different arrays of fibres are also considered.

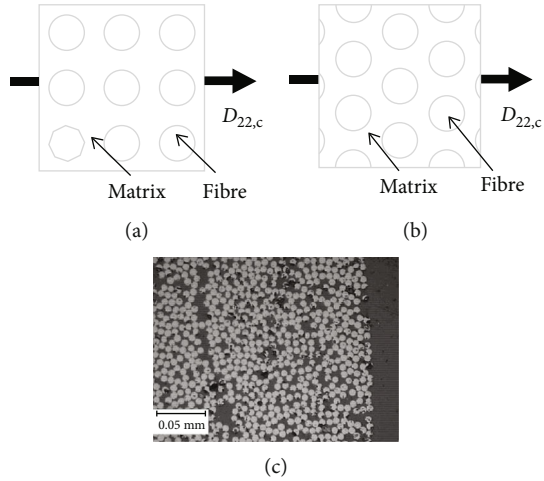

Figure 1: (a) Square array packing and (b) hexagonal array packing (c) 500× magnified optical microscope image of CFRP tendon edge.

The Keller and Sachs model [34] assumes fibres are squarely packed in a regular array as shown in Figure 1(a). Using symmetry, this system can be reduced to one quarter of an element consisting of a single circular fibre and surrounding matrix (see Figure 2(a)). The ratio of fibre area to the total element area is equal to the volume fraction of the composite considered. The diffusivity through the fibre is taken as zero, and so, the transverse diffusivity $D_{22,c(\mathrm{KS})}$ is approximated as

$$\frac{D_{22,c(\mathrm{KS})}}{D_e} = \left[1 + \frac{2V_f}{1 - V_f - 0.30584V_f^4 - 0.013363V_f^8}\right]^{-1}, 0 \le V_f \le 0.55$$
$$= \left[\pi\left[2\left(1 - 2\sqrt{\frac{V_f}{\pi}}\right)\right]^{-1/2} - 1.95\right]^{-1}, 0.55 \le V_f \le \pi/4. \quad (6)$$

When V_f equals $n/4$, it is presumed that the edges of the fibres in the square array are touching, preventing solution from passing, thereby reducing the modelled diffusivity of the composite to zero.

The parallel-series approximation [35] splits the element into thin layers perpendicular to the direction of diffusion as shown in Figure 2(b). The common interpretation of the model assumes cylindrical impermeable fibres. An effective diffusivity for each layer, d_p, is calculated, and the layers are summed in series to obtain the transverse diffusivity of the composite, according to the series equation given by Crank [27], where

$$\frac{b/2}{D_{22,c}} = \sum \frac{dx}{d_p}. \quad (7)$$

The diffusivity for each strip is a function of the ratio of fibre and matrix proportions, where

$$d_p = \frac{D_e(b/2 - y) + D_f y}{b/2} \approx \frac{D_e(b - 2y)}{b}. \quad (8)$$

Substitution of Equation (8) into (7) followed by integration yields:

$$\frac{D_{22,c(\mathrm{PS})}}{D_e} = \left[1 - 2\sqrt{\frac{V_f}{\pi}} - \frac{1}{2}\left\{\pi - \frac{4}{\sqrt{1 - 4V_f/\pi}} \tan^{-1}\frac{\sqrt{1 + 2\sqrt{V_f/\pi}}}{\sqrt{1 - 2\sqrt{V_f/\pi}}}\right\}\right]^{-1}, \frac{4V_f}{\pi} < 1. \quad (9)$$

As it is assumed that every strip can transport flux to some extent, this represents an upper bound.

The series-parallel approximation [35] splits the element into thin layers parallel to the direction of diffusion, as shown in Figure 2(c). An effective diffusivity for each layer, d_s, is calculated based on the series equation by Crank [27]

$$\frac{b/2}{d_s} = \frac{x}{D_e} + \frac{b/2 - x}{D_f} \Rightarrow d_s = \frac{c}{2}\left(\frac{D_e D_f}{D_e c/2 - (D_e + D_f)x}\right). \quad (10)$$

And the layers are summed in parallel to obtain the transverse diffusivity of the composite, using

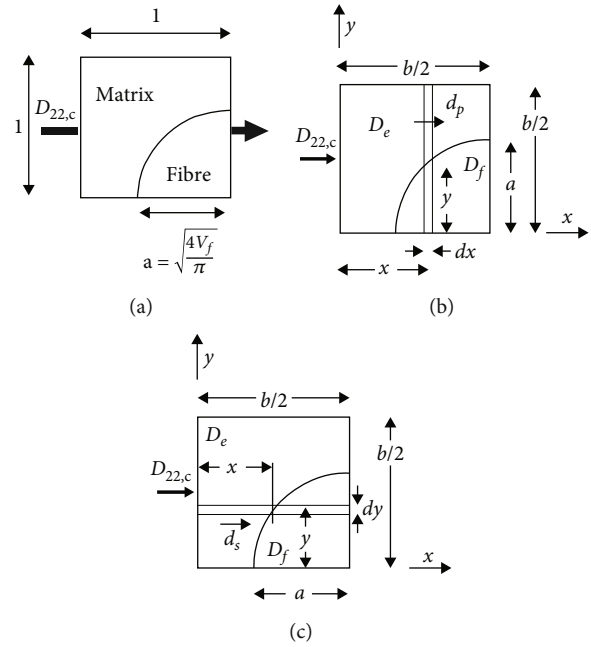

FIGURE 2: (a) Repeating element of a composite used in the Keller-Sachs, SP, and PS models, (b) Parallel-series (PS) approximation and (c) series-parallel (SP) approximation to the transverse diffusivity of a composite element.

$$\frac{D_{22,c(\mathrm{SP})}}{D_e} = 1 - 2\sqrt{\frac{V_f}{\pi}}. \tag{11}$$

This model suggests that any strip that includes part of a fibre is assumed to have a diffusivity of zero. As a result, this model is a lower bound. Nevertheless, it is extensively used in the literature [8, 22, 33, 36] given its ease of implementation.

To determine the influence of the assumed packing array, finite element analyses were undertaken by Kondo and Taki [32] and Bond [10]. For a repeating unit of a square (see Figure 1(a)) or hexagonal (see Figure 1(b)) array of fibres, the transverse diffusivity was evaluated in the same manner as Keller and Sachs. However, rather than expressing transverse diffusivity mathematically, finite element analyses were used to consider the steady state flow through a repeating unit of an array of fibres. Bond [10] simulated both diffusion through an array of hexagonally arranged fibres and an array of randomly spaced fibres but found the randomness of fibre spacing had no effect on the transverse diffusivity of the composite except at high fibre-volume fractions.

4. Evaluation of Transverse Diffusivity Models

The variation of $D_{22,c}/D_e$ is plotted in Figure 3 for increasing volume fractions based on the models discussed in the previous section; the Keller-Sachs, PS, and SP models were calculated numerically, whereas the values for the Kondo and Taki [32] and Bond [10] models were referenced from their above mentioned papers. Experimental results conducted by others [9, 10, 22, 24, 32, 35, 37–41] are used to compare the diffusivity of the epoxy to the transverse diffusivity of the corresponding carbon fibre composite and have been superposed on the model predictions. The experiments have been carried out under a number of different conditions, as listed in Table S1. The composite specimens studied were all laminates with an epoxy matrix. The majority of the moisture uptake experiments were conducted at high humidity conditions ≥85%) or in water immersion. The accelerated ageing temperatures ranged from 27-121°C with the maximum value adopted in Shen and Springer [9].

As noted, the SP approach represents a lower bound but rather unexpectedly, the Kondo and Taki square array predictions are greater than the anticipated upper bound PS approach. In terms of the influence of the packing arrangement, at lower volume fractions, the nature of the assumed array appears to be insignificant, but higher diffusivity is associated with the hexagonal array at larger volume fractions. Figure 3 also shows, as expected, that the solution obtained by Bond [10] for the square array is similar to that of the Keller-Sachs approximation. In most instances, the experimental $D_{22,c}/D_e$ results exceed the predications, with the exception of the models proposed by Kondo and Taki. The finite element analysis by Kondo and Taki for a square array of fibres overestimates, and the parallel-series model underestimates the transverse diffusivity for the majority of the experimental results. Deviations in the FEA results between the Kondo and Taki [32] and Bond [10] models are observed. The reasons for these deviations are unclear but could possibly be attributed to differences in the typical repeating unit, boundary conditions, and degree of discretisation in the FEA models. There are no obvious trends in the relationship between the experimental $D_{22,c}/D_e$ and V_f. Scatter exists not only between differing investigations but also within sets of experimental results. A large part of the

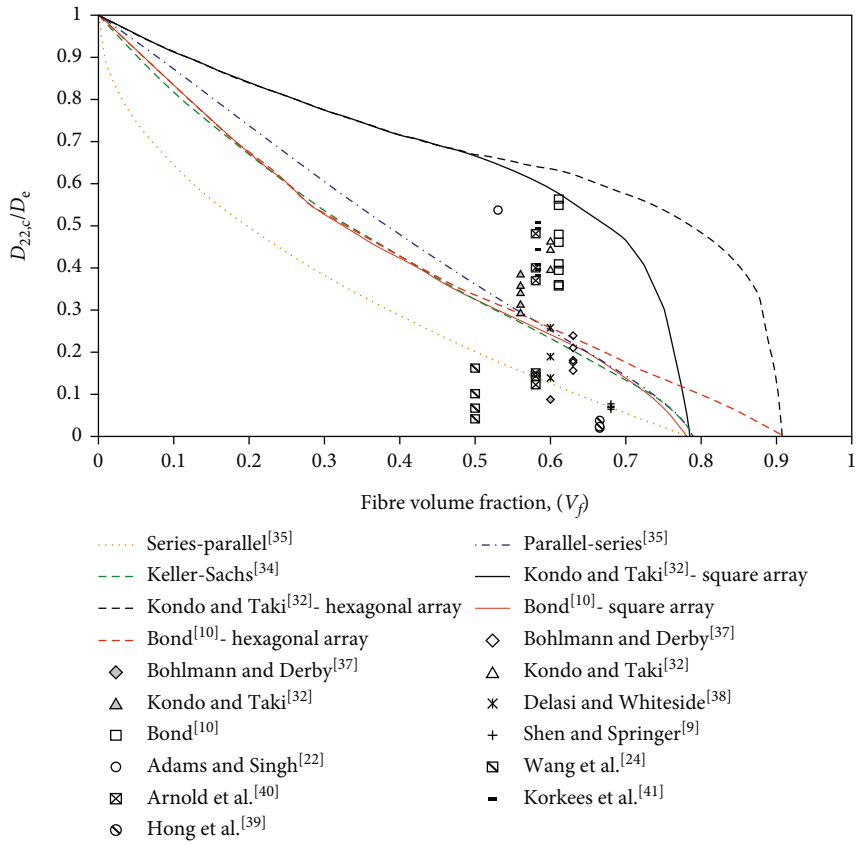

Figure 3: Comparison of experimental and modelled transverse diffusivities.

Table 1: ANOVA F-test analysis for different variables affecting $D_{22,c}/D_e$.

Variable	F	p value	F_{crit}
V_f ([0.5-0.6], [0.6-0.7])	0.50	0.481	4.04
T ([23–30], [50-60], [65-70], [75-100])	3.48	0.024	2.83
T ([23–30], [50-60], [65-75], [80-100])	3.39	0.027	2.83
RH ([96-100], [85-96], [65-75], [20-60], [water])	3.91	0.008	2.58
RH ([90-100], [65-85], [20-65], [water])	2.86	0.047	2.81

Note: V_f: fibre volume fraction; T: temperature; RH: relative humidity; []: group range.

experimental scatter between different investigations may be due to differences in materials, test conditions, specimen geometry, and diffusion modelling, and none of which are standardised.

To further investigate possible trends according to key parameters such as temperature and exposure conditions, an ANOVA F-test analysis was carried out. These results have been summarised in Table 1 and will be discussed further in the next section.

4.1. Temperature and Solution Exposure. Temperature (to facilitate accelerated ageing testing) and solution exposure (to simulate a marine environment) are parameters of particular interest in the current work. Although the diffusivities of the epoxy and the composite would be expected to increase with temperature [42–44] and humidity [30, 45], this does not necessarily mean the value of $D_{22,c}/D_e$ will also increase. The experimental $D_{22,c}/D_e$ values from the Table S1 were grouped within different ranges of temperature and exposure conditions. A one-way ANOVA F-test analysis was carried out to understand if the subgroups are statistically significantly different from each other (significance level 0.05). A higher level of statistical significance among groups is indicated by $p < 0.01$. To minimise bias, different groups were considered at each temperature and humidity parameter. The ANOVA results suggest that the RH exposure conditions affect the $D_{22,c}/D_e$ at a higher number of subgroups ([96-

Table 2: Properties of epoxy resin and CFRP tendons studied.

Property	Value
Fibre type	Tenax UTS 5631
Matrix type	EPR 4434/EPH 943
Resin: hardener mixing ratio	Proprietary data
Resin cure cycle	Proprietary data
Volume fraction, V_f	0.64
Tendon diameter, d (mm)	5.4
Surface coating	Quartz sand, 0.4–0.63 mm diameter grains
Tensile strength (MPa)	1,913
Glass transition temperature (°C)	135.5–145 (DMTA[a)])

[a)]: dynamic mechanical analyzer.

100], [85-96], [65-75], [20-60], and [water]) with $p < 0.01$. The temperature has a minor effect on the transverse diffusivity (F values close to F_{crit} and $0.01 < p < 0.05$) regardless the subgroups considered.

Bond [10], Shen and Springer [9], and Abanilla and Karbhari [36] found that the transverse diffusivities of the composites changed with temperature at the same rate as the matrix diffusivity indicating temperature had little effect on the $D_{22,c}/D_e$ or $D_{11,c}/D_e$ ratios. This is in contrast to the findings of Blikstad [7] who found that the relative diffusivities varied with temperature. Bond [10] noted a positive correlation between moisture concentration and transverse diffusivity and attributed this to the effect of moisture concentration on the size of the fibre-matrix interphase region surrounding the fibres, a region to which Bond attributed increased diffusivity.

4.2. Diffusion Modelling. The accuracy of the diffusion modelling used to evaluate the $D_{22,c}/D_e$ ratio is important. Use of Fickian modelling rather than more accurate anomalous diffusion modelling was shown to increase scatter in the results by 60% [10]. In Table S1, the majority of the studies employed Fickian models, yet in many cases, the exact nature of the behaviour is not reported nor is it confirmed that saturation has been reached, and hence, the assumed mass at saturation and the accuracy of the $D_{22,c}/D_e$ calculations is then difficult to ascertain. Nevertheless, even the anomalous diffusion modelling undertaken by Bond [10] produced a series of results with considerable scatter. This suggests that limitations in modelling accuracy are not solely responsible for the spread of data observed. Moreover, the real distribution of carbon fibres deviates from a perfectly square and hexagonal array, and a random distribution of resin rich, resin-poor areas, and fibre-to-fibre contact is more representative as observed with microscopy. Bond [10] showed that the addition of an extra thin resin layer in his model could yield $D_{22,c}/D_e$ values closer to the lower end of the experimental findings. Moreover, the accumulation of fibre-matrix interphases when fibres are at close proximity can greatly affect the diffusivity values and lead to higher scatter [46].

5. Experimental Programme, Chemical Data, and Material Data

To probe the relationship between the diffusion of epoxy thin films and companion cylindrical carbon epoxy tendon composites, an experimental programme was undertaken. Moisture uptake experiments were conducted in CFRP tendons and are presented here. These results are compared and benchmarked against moisture uptake findings of epoxy thin films of the same matrix as in the CFRP tendons presented in Scott and Lees [28] as part of the same experimental programme. The samples were immersed in salt water solution, and two different temperatures were used to assess the effect of elevated temperatures on solution uptake and transverse diffusivity.

5.1. Material Properties. Resin thin films were prepared based on the ASTM standard D823-087 [47] and using the same epoxy-amine (EPR 4434/EPH 943) thermoset system of the reference CFRP tendons. The films had nominal dimensions of $38 \times 18 \times 0.34$ mm and were cured in an oven using the vacuum bagging process. A similar curing regime to that of the CFRP tendons was adopted. The exact details of the curing process are confidential, but a maximum temperature of 195°C was applied. More details on the epoxy thin film preparation can be found in Scott and Lees [28]. Differential scanning calorimetry (DSC) tests on the resin film samples yielded glass transition temperatures, T_g, of 132.9°C and 141.0°C in the same range of the nominal values quoted by the manufacturer. Moisture absorption experiments were then conducted on these analogous epoxy thin samples that were submersed in a salt water solution [28]. The experiments were used to ascertain Fickian and Langmuir uptake parameters for the pure epoxy at 20°C and 60°C [28].

The nominal chemical and mechanical properties specified by the manufacturers for the epoxy-amine (EPR 4434/EPH 943) 5.4 mm diameter CFRP tendons are listed in Table 2. One complication with the CFRP tendons as supplied was the presence of a sand coating to increase the bond between the CFRP tendon and concrete. The sand particles are embedded in an additional resin rich layer on the tendon

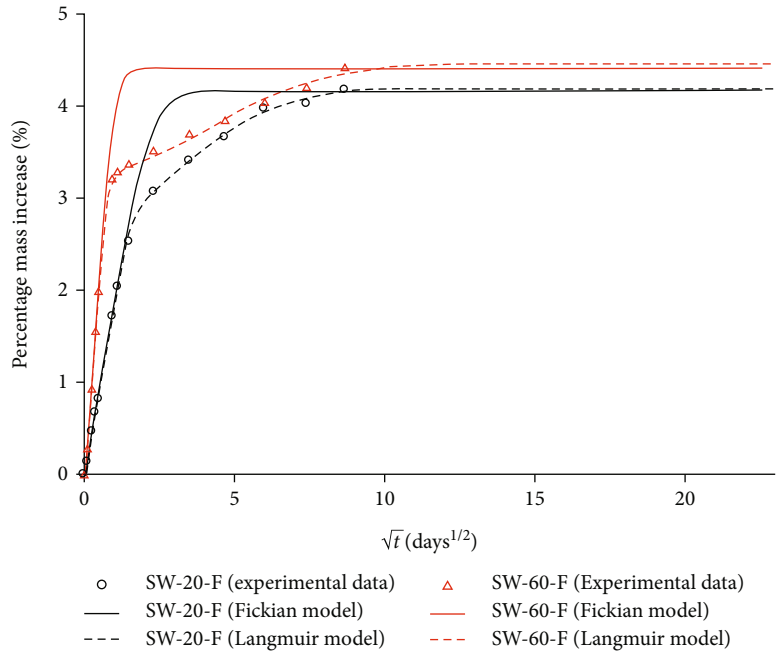

Figure 4: Mass uptake in pure epoxy at 20°C and 60°C. Reproduced with permission (Copyright Wiley Online Library, 2013).

surface. Since the coating represented a further variable, it was felt to be prudent to use a blade to manually scrape off the sand and the glossy resin rich layer. This method was chosen since the only forces applied to the material were small and unlikely to cause internal damage. The tendons were then cleaned using acetone. Five diameter readings were taken at distinct axial and hoop positions on each specimen using a micrometer at 20°C. Taking into account all the sections tested, the mean specimen diameter was 5.448 mm.

5.2. Moisture Absorption Tests. Moisture uptake tests were conducted on CFRP tendons after immersion in salt water solution at either 20°C or 60°C. Three specimens cut to a length of 150 mm were considered at each temperature. This length such that the effect of any axial diffusion through the material was not significant, e.g., albeit for a vinyl ester matrix. Gagani et al. [25] showed that axial diffusivity was only a factor in CFRP rods (with a 6 mm diameter) shorter than 30 mm. The tendons were initially dried in the oven at 60°C and subsequently submerged into a polypropylene sealed flask containing one litre of salt water solution comprised of 3.5% by mass sodium chloride and deionised water. The materials were weighed to within 0.1% of their nominal values and mixed until homogeneous. The flasks were either kept in a temperature-controlled lab at 20°C or maintained at 60°C in a temperature-controlled oven. The maximum temperature is lower than the maximum recommended value of 80°C in ASTM D5229/D5229M-20 [48] for epoxies cured at 177°C and is also lower than the saturated T_g value of equivalent CFRP tendons (diameter = 4.2 mm) with the same epoxy/hardener system and curing regime, where $T_{g\text{–onset–wet}} = 86.6$°C [49].

Gravimetric sorption was used to measure the solution uptake in the tendon and epoxy film samples. Mass readings were taken using a Mettler AE160 balance of 0.1 mg resolution. At each time interval, the samples were removed from the solution, rinsed in deionised water, blotted dry, and then weighed before being returned to solution. The mass increase at time t was calculated using

$$M_t = 100\left[\frac{m_t - m_o}{m_o}\right], \tag{12}$$

where m_t is the mass reading after exposure time t and m_o is the dry mass of the sample.

6. Experimental Results and Diffusion Modelling

The experimental and predicted mass uptakes plotted against the square root of time are shown in Figure 4 for the epoxy thin films. The notation adopted is *A-B-C*, where *A* denotes the salt water solution (SW), *B* indicates the exposure temperature (20 and 60°C), and *C* represents the sample (*F* is film and *T* is tendon).

For the CFRP tendons, the experimental mass uptake readings with respect to the square root of time are shown in Figure 5(a). Each data point represents the average for three specimens for the 20°C and 60°C experiments, respectively. Early-stage readings were taken regularly during a period of up to around 25 days, and later stage readings were acquired after nearly 2 years and 4.5 years. The error bars illustrate 95% confidence limits based on the standard error of the mean, assuming a normal distribution of data. The

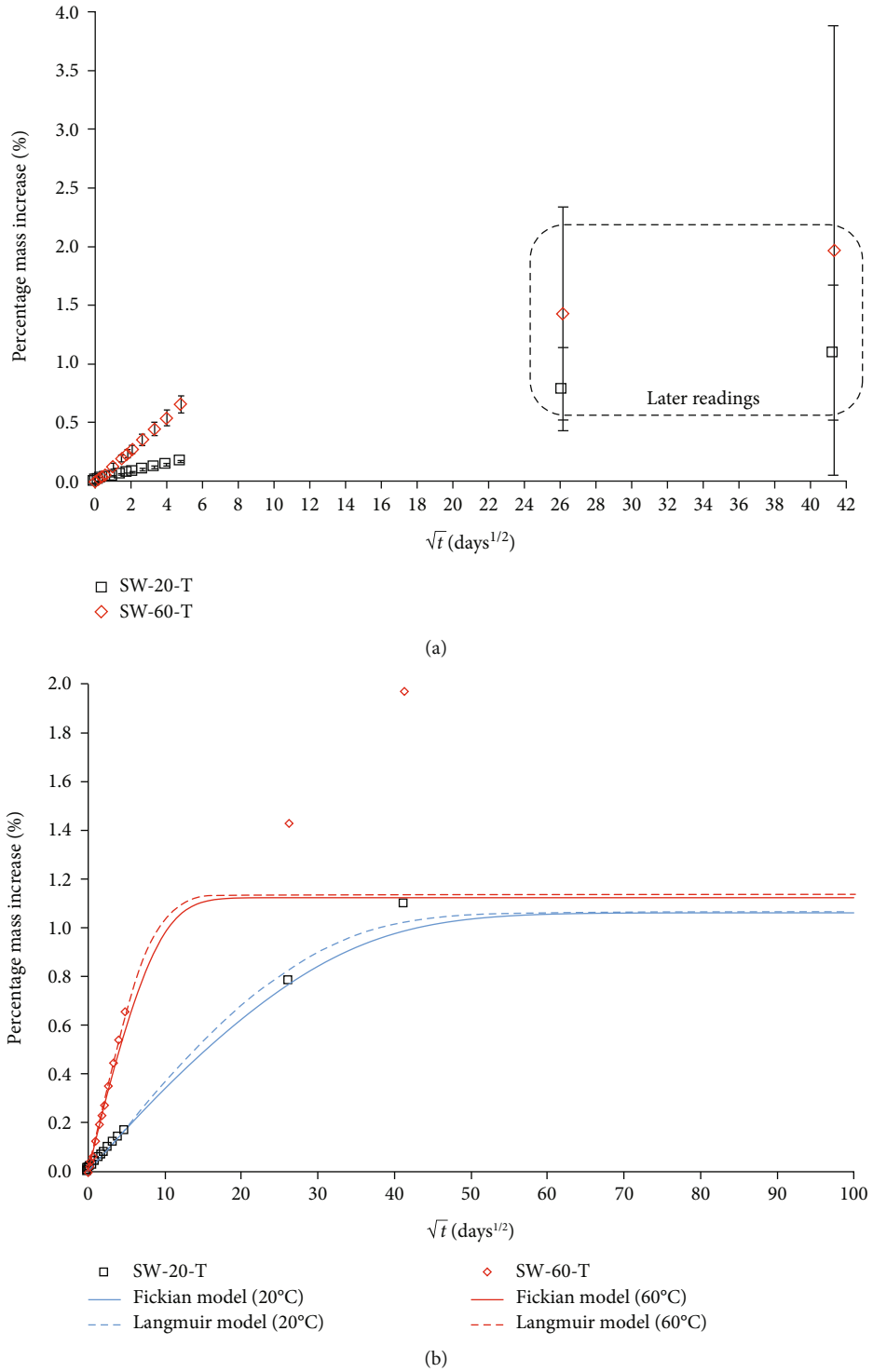

Figure 5: (a) Mass uptake in CFRP tendons at 20°C and 60°C and (b) Fickian and Langmuir modelling.

error bars for the uptake at 60°C are considerably larger than those at 20°C and tend to increase with increasing exposure time. The variability in mass readings increases at longer exposure times (after 685 days) and particularly at 60°C suggesting that additional degradation phenomena take place in a few outliers. The mass uptake at saturation has not been attained even after 1710 days ($\sqrt{t} = 41.4\,\text{days}^{1/2}$) of exposure in salt water, although firm conclusions cannot be derived due to the high scatter in later readings.

6.1. Diffusion Modelling. For the epoxy thin films, the Fickian diffusion coefficient parameters were calculated according to Crank [27] from the initial linear slope of the experimental data using the last mass reading for the mass

Table 3: Epoxy thin film Fickian and Langmuir diffusion parameters at 20°C and 60°C.

Parameter	20°C	60°C
Fickian mass uptake at saturation, $M_{\infty,e,F}$ (%)	4.174	4.416
Fickian solution concentration at saturation, $C_{0,e,F}$ (mol/cm^3)	0.002453	0.002596
Fickian diffusion coefficient of epoxy, $D_{e,F}$ (cm^2/day)	4.820×10^{-5}	2.187×10^{-4}
Mass uptake at Langmuir saturation, $M_{\infty,e,L}$	4.188	4.470
Langmuir solution concentration at saturation, $C_{0,e,L}$ (mol/cm^3)	0.002462	0.002628
Langmuir diffusion coefficient of epoxy, $D_{e,L}$ (cm^2/day)	1.095×10^{-4}	4.008×10^{-4}

Table 4: CFRP tendon Fickian and Langmuir-diffusion parameters at 20°C and 60°C.

Parameter	20°C	60°C
Fickian solution concentration at saturation, $C_{0,c,F}$ (mol/cm^3)	0.0008832	0.0009344
Fickian mass uptake at saturation, $M_{\infty,c,F}$ (%)	1.061	1.123
Fickian-diffusion coefficient parallel to fibre direction, $D_{11,c,F}$ (cm^2/day)	1.735×10^{-5}	7.874×10^{-5}
Fickian-diffusion coefficient transverse to fibre direction, $D_{22,c,F}$ (cm^2/day)	1.735×10^{-5}	2.165×10^{-4}
Langmuir solution concentration at saturation, $C_{0,c,L}$ (mol/cm^3)	0.0008863	0.0009461
Mass uptake at Langmuir saturation, $M_{\infty,c,L}$ (%)	1.065	1.137
Langmuir-diffusion coefficient parallel to fibre direction, $D_{11,c,L}$ (cm^2/day)	3.942×10^{-5}	1.443×10^{-4}
Langmuir-diffusion coefficient transverse to fibre direction, $D_{22,c,L}$ (cm^2/day)	3.285×10^{-5}	4.770×10^{-4}

uptake at saturation, $M_{\infty,e,F}$. The Langmuir diffusion parameters were calculated using nonlinear regression analysis (please see Scott and Lees [28] for further details). The Fickian and Langmuir diffusion parameters of the epoxy thin films are summarised in Table 3, and the relevant analytical results are superposed in Figure 4. The experimental uptake in the thin films was non-Fickian and more accurately modelled using a Langmuir approach.

As it appeared, as if the CFRP tendons had not yet saturated even after 4.5 years, the thin film concentration at saturation parameters shown in Table 3 were used in Equations (3) and (4) to predict the mass uptake at saturation for the composite. The resulting values for both Fickian and Langmuir diffusion are summarised in Table 4. It should be noted that these are values of average concentration per unit volume of the composite studied whereas in reality, the solution concentration will tend towards a higher value in the matrix, but will be zero in the fibres. A caveat to this relationship, as with all the discussed modelling, is the assumption that the composite is free from voids and is of sound fibre/matrix bond.

The diffusivity parallel to the fibre direction, $D_{11,c}$ was calculated from Equation (5), and included in Table 4 where the CFRP tendon Fickian and Langmuir diffusion parameters denoted as $D_{11,c,F}$ and $D_{11,c,L}$, respectively. The transverse Fickian-diffusion coefficient, $D_{22,c,F}$, of the CFRP tendons was calculated based on a MATLAB [50] script and an iterative process, where different diffusion coefficient values were applied in Equation (2). The diffusion coefficients were derived by adopting different knockdown factors in the epoxy Fickian-diffusion coefficient, $D_{e,F}$. The solution was obtained when the error between the Fickian predicted and experimental mass uptake values was minimised. The calculation of the diffusion coefficient, $D_{22,c,F}$, from the linear slope of the M_t versus $\sqrt{t}$ experimental data according to Crank [27] is more accurate when $M_t \leq 0.6\, M_{\infty,c}$ and is not as robust for cylinders as for plane sheets [27]. Therefore, the methodology mentioned above was judged to be more accurate. The Langmuir-diffusion coefficient, $D_{22,c,L}$, was derived following a similar iterative process by applying various knockdown factors in the epoxy Langmuir-diffusion coefficient, $D_{e,L}$. A finite difference simulation was adopted for the radial Langmuir diffusion, and the mass uptake was derived by integration of the resulting concentration gradients. More details of the methodology can be found in Scott [31].

The Fickian and Langmuir predictions are shown in Figure 5(b). The two model predictions are fairly similar for the tendons even though the thin film behaviour was distinctly anomalous (cf. Figure 4). In addition, the Langmuir modelling of radial diffusion does not predict an upward drift at intermediate times which was observed in the thin film modelling. This has also been observed elsewhere [12]. As the through-thickness dimensions increase, the concentration gradients of the bound molecules become similar in profile to that of the free molecules. This implies that a simpler, Fickian model maybe adequate for representing diffusion in FRP prestressing materials which will typically have diameters >4 mm.

Both the Langmuir and Fickian predicted mass uptake values at 20°C agree fairly well with the experimental data after 686 ($\sqrt{t} = 26.2$ days$^{1/2}$) and 1710 days ($\sqrt{t} = 41.4$ days$^{1/2}$) of exposure and the predicted mass at saturation ($M_t = 1.06\%$) is similar to the average experimental mass

uptake after 1710 days. Both models predict well the mass uptake at 60°C at short exposure time, but considerable deviations occur at longer exposure. The average experimental mass uptake at 60°C is approximately 70% higher than the predicted value after 1710 days ($\sqrt{t} = 41.4\,\text{days}^{1/2}$). This increased mass uptake at 60°C can be attributed to either secondary cross-linking of bound water molecules that is facilitated at elevated temperature [14] or to degradation phenomena at the fibre/matrix interface. The latter will be explored in Section 7.

6.2. $D_{22,c}/D_e$ Ratios. In Table 5, the experimentally derived knockdown factors based on the ratio of the CFRP and epoxy thin film diffusion parameters are shown. For 20°C exposure, the best fit $D_{22,c}/D_e$ ratio was found to be 0.36 and 0.30 for the Fickian and Langmuir models, respectively. For 60°C exposure, the corresponding values were found to be 0.99 and 1.19 for the Fickian and Langmuir models, respectively. This is counterintuitive given that the presence of fibres in an epoxy would be expected to decrease rather than increase the transverse diffusivity through the material.

The transverse diffusivity $D_{22,c}$ of the CFRP tendon as predicted by the Keller-Sachs (Equation (6)), the parallel-series (Equation (9)), the series-parallel (Equation (11)), and mathematical models are presented for the Fickian and Langmuir-diffusion models for 20°C and 60°C shown in Table 5. The models are temperature independent, so the same $D_{22,c}/D_e$ factor applies for both temperatures. Even the highest knockdown factor (parallel-series, $D_{22,c}/D_e = 0.2086$) is an underestimate.

6.3. Comparison of Calculated $D_{22,c}/D_e$ Ratios with Values in the Literature. Figure 6 compares the values of $D_{22,c}/D_e$ at 20°C and 60°C for the CFRP tendons studied, calculated using either the Fickian and Langmuir models. The $D_{22,c}/D_e$ ratio at 20°C is consistent with the bulk of results in the literature, and whether Fickian or Langmuir modelling is used made little difference. The results at 60°C, however, are higher than expected.

7. Discussion

The relatively high $D_{22,c}/D_e$ in the composite at 60°C suggests that there may be damage occurring, or that the fibre-matrix interface becomes a factor in wet conditions at elevated temperatures. Considering that elevated temperatures accelerate the ageing process without inducing any additional degradation according to the Arrhenius principles, the $D_{22,c}/D_e$ ratio should be the same regardless the temperature regime. The exposure temperature at 60°C should increase the tendon diffusion value by a factor of 13 compared with the exposure temperature at 20°C based on the Arrhenius principles and

$$D_{22,c}(T) = D_0 e^{(-E_a/\text{RT})}, \tag{13}$$

where $D_{22,c}(T)$ is the diffusion coefficient at temperature T, D_0 is a preexponential factor having the same units as $D_{22,c}(T)$, $E_a = 51367$ Joules/mol is the activation energy as calculated in Toumpanaki et al. [51] for the same material, $R = 8.314$ Joules/Kmol is the molar gas constant, and T is the temperature in Kelvin.

The experimental $D_{22,c,F}$ and $D_{22,c,L}$ values at 60°C are 12.5 and 12.1 times higher than the respective ones at 20°C and correlate well with the predictions based on Equation (13). However, the experimental $D_{e,F}$ and $D_{e,F}$ values at 60°C are 4.5 and 3.7 times higher than the corresponding ones at 20°C resulting in $D_{22,c}/D_e$ values at 60°C in the range of 3-4 compared with the relevant values at 20°C. Assuming that the activation energy E_a is a matrix dominated property since the diffusion process is a matrix dominated property and it is the same for both the epoxy thin films and CFRP tendons, the $D_{22,c}/D_e$ values at elevated temperature should be unit values based on the Arrhenius principles, and the higher values observed experimentally suggest that additional degradation phenomena take place.

Joliff et al. [20] measured glass transition temperatures in the range of 40-110°C in the fibre/matrix interphase area of GFRP laminates with the lowest values being recorded at the vicinity of the fibres. Assuming an equivalent glass transition temperature in the interphase area of the CFRP rods, the commonly applied accelerated ageing temperature of 60°C is expected to have degraded the fibre-matrix interface where the softening temperature is below 85°C (leaching of the softer interphase). To explore whether a region of a higher diffusivity around the fibre is a plausible explanation, the parallel-series approach (Equation (9)) was modified to include an additional interphase region with a thickness t_i and a diffusivity D_i as shown in Figure 7(a). In the region from x to the edge of the matrix-interphase region, the diffusivity of a strip is taken as that of the matrix. Thereafter, the diffusivity of a strip can be expressed as

$$d_p = \frac{D_e(b/2 - t_y - y) + D_i t_y + D_f y}{b/2} = \frac{D_e(b - 2t_y - 2y) + 2D_i t_y}{b}, \tag{14}$$

where $D_f = 0$, $y = 0$ when $x < (b/2 - a)$, and $t_y = 0$ when $x < (b/2 - (a + t_i))$.

This expression has been plotted as a function of increasing volume fraction in Figure 7(b) for four cases where $t_i = 0.05\,a$, $t_i = 0.1\,a$, $D_i = 4\,D_e$, and $D_i = 10\,D_e$. The assumed thickness of the interphase area for a Tenax carbon fibre ($a = 7\,\mu$m) is within the range of microscopic observations in Gagani et al. [25] and Joliff et al. [20] for CFRP and GFRP rods, respectively. It can be seen that the possibility of an interphase region with an increased diffusivity can have a significant impact on the calculated value of $D_{22,c}$. As the total volume of the interphase would be expected to be a function of the V_f, it is of note that this region becomes of increasing importance with a higher volume fraction. Values of $D_{22,c}/D_e > 1$ can be noted when the thickness of the interphase region is $0.1\,a$ and the relative diffusivity is $10\,D_e$. The experimental $D_{22,c}/D_e$ values for the SW-60-T group agree better with the model predictions assuming an interphase region with a higher diffusivity $D_i = 10D_e$. An interphase region with a diffusivity in the range of $D_i = (1.0 - 4.0)\,D_e$

Table 5: Comparison of transverse Fickian and Langmuir diffusion-coefficient models at 20°C and 60°C exposure.

Specimen	Diffusion model				Parallel-series	Series-parallel	Keller-Sachs	Best fit using experimental data
				$D_{22,c}/D_e$	0.2086	0.09730	0.1934	
SW-20-T	Fickian	D_e (cm^2/day)	4.820×10^{-5}	$D_{22,c,F}$ (cm^2/day)	1.006×10^{-5}	4.690×10^{-6}	9.323×10^{-6}	1.735×10^{-5} ($D_{22,c}/D_e = 0.36$)
	Langmuir	D_e (cm^2/day)	1.095×10^{-4}	$D_{22,c,L}$ (cm^2/day)	2.284×10^{-5}	1.065×10^{-5}	2.118×10^{-5}	3.285×10^{-5} ($D_{22,c}/D_e = 0.30$)
SW-60-T	Fickian	D_e (cm^2/day)	2.187×10^{-4}	$D_{22,c,F}$ (cm^2/day)	4.563×10^{-5}	2.128×10^{-5}	4.230×10^{-5}	2.165×10^{-4} ($D_{22,c}/D_e = 0.99$)
	Langmuir	D_e (cm^2/day)	4.008×10^{-4}	$D_{22,c,L}$ (cm^2/day)	8.361×10^{-5}	3.900×10^{-5}	7.751×10^{-5}	4.770×10^{-4} ($D_{22,c}/D_e = 1.19$)

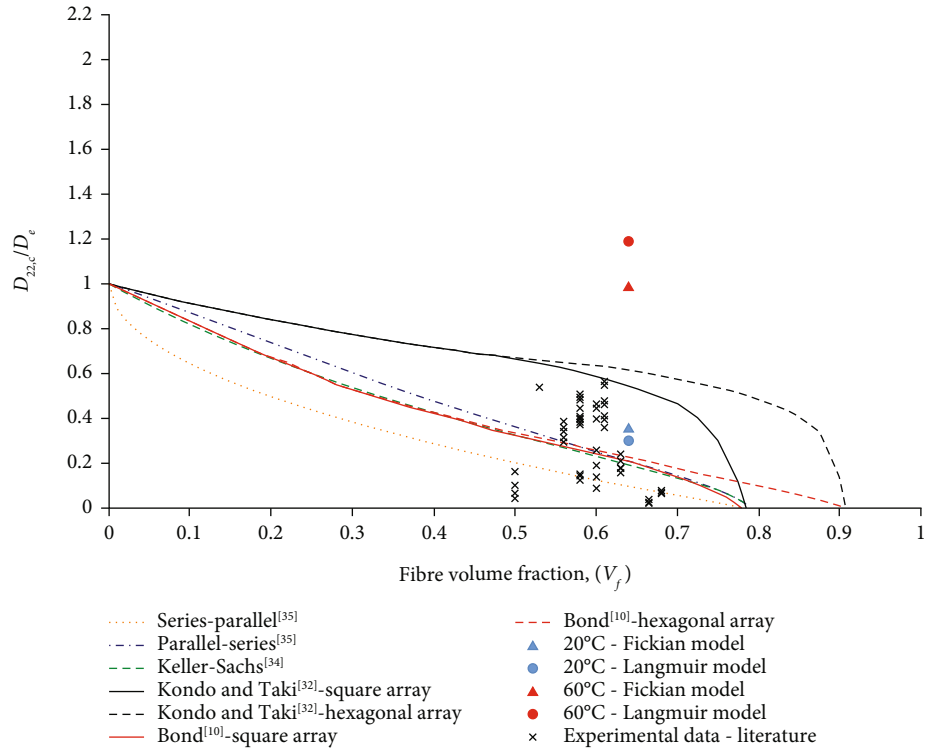

Figure 6: Calculated values of transverse diffusivities compared to findings in the literature.

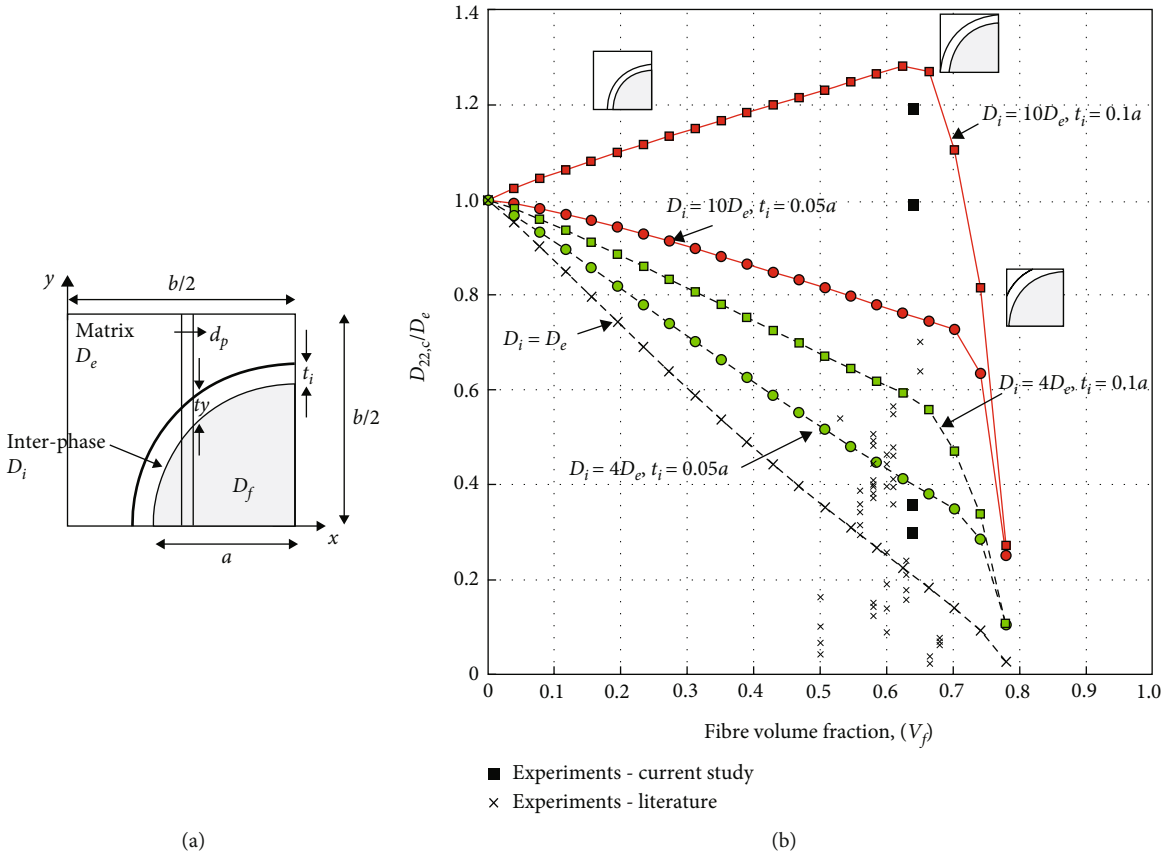

Figure 7: (a) Repeating element of a composite with an interphase region and (b) transverse diffusivity values as a function of interphase properties (thickness, t_i, and diffusion, D_i).

yields $D_{22,c}/D_e$ values similar to the best-fit experimental ones of the SW-20-T group. The adopted higher diffusivity values, D_i, are in general agreement with numerical studies in Joliff et al. [20] and Rocha et al. [46] to study the effect of interphase area in the moisture uptake of GFRP laminates, e.g., Joliff et al. [20] adopted an interphase area of 4 μm thickness and $D_i = 10\,D_e$ to better fit the numerical moisture uptake findings in deionised water at 70°C. However, the approach presented here is a simpler method of calculating the bulk tendon diffusion coefficient accounting for the interphase area in lieu of the trial and error methodology in ABAQUS FE simulations to fit experimental with numerical findings [20].

A further experimental parameter that may be causing considerable uncertainty in the modelling is the percentage mass increase at saturation. The modelling has assumed that the solution concentration in the composite is proportionally related to the solution concentration in the pure matrix specimens and the volume fraction. However, as discussed, experimental studies by others [10] have indicated that the mass uptake at saturation in a composite cannot solely be described by Equations (3) and (4). The result of this anomaly is that if incorrect solution concentrations are being specified at the surface, incorrect diffusion coefficients will be specified when attempting to obtain a least squares fit between the experimental results and the percentage mass increase calculated from the erroneous concentration gradients. Adopting the latest mass uptake reading from short-term experimental moisture uptake data in CFRP tendons may result in an inherent uncertainty regarding the assumed required time to reach saturation. The mass at saturation is independent of the accelerated ageing temperature [15, 48], but degradation phenomena at elevated temperature that lead to increased values compromise the accuracy in moisture uptake predictions. The adoption of the last experimental mass uptake reading at elevated temperatures in lieu of the mass at saturation may lead to erroneous conclusions. Fickian predictions at longer exposure times may fit better with experimental data but may represent bulk moisture uptake predictions that cannot capture the any wicking phenomena due to degradation or the presence of voids at the fibre/matrix interface.

All data found in the literature and presented in Figure 7(b) refer to either full immersion in water or exposure at high humidity levels, and the experimental $D_{22,c}/D_e$ values in this study refer to full immersion in salt water. Firm conclusions on the effect of salt water in the diffusivity of epoxies have not been derived, and experimental results depend on the epoxy chemistry and curing conditions but also exposure temperature [28]. Abanilla et al. [36] reported similar mass at saturation when carbon/epoxy laminates were exposed at deionised and salt water solution at 23°C for 100 weeks. However, higher diffusion coefficient values were derived after exposure in salt water attributed to a straining effect from clustering of NaCl particles at the surface. The epoxy thin films in this study were exposed in water at both 20°C and 60°C in Scott and Lees [28] and exhibited similar mass at saturation and diffusion coefficient values with the samples exposed in salt water. It is therefore plausible that the CFRP tendons studied here have similar diffusivity behaviour in both water and salt water.

The possibility of predicting long-term diffusion behaviour of CFRP tendons using short-term studies of the epoxy matrix has been demonstrated to an extent. Although most studies in the literature consider unidirectional flow through composites, Fickian and Langmuir principles can be applied to the radial uptake in a three-dimensional CFRP cylinder. Temperature can be used as a means of acceleration, however, the work carried out here and studies reviewed in the literature have shown that temperature, particularly in combination with a wet environment, may alter the nature of diffusion in composites. It seems to be necessary to study absorption in both the epoxy and the composite in order to establish the long-term behaviour in the tendon, given the limited effectiveness of the transverse diffusivity models. Observing actual values of saturation in both the epoxy and the composite are keys in the assessment of accurate diffusion parameters.

8. Conclusions

An investigation was undertaken to measure and predict the long-term salt water uptake in cylindrical CFRP tendons used in prestressed concrete applications. Experiments were conducted where CFRP tendons were exposed to salt water solutions at 20°C and 60°C. The tendon diffusion parameters were then compared with previous thin film epoxy results. The combination of salt water exposure and temperature was found to have a significant effect on the $D_{22,c}/D_e$ ratio. At 20°C, the observed $D_{22,c}/D_e$ ratio was similar to values reported by others in the literature, but at 60°C, the transverse diffusivity of the composite was similar to that observed in the matrix. The predicted results using a parallel-series approach were found to be particularly sensitive to the presence of an interphase region with increased diffusivity and also the assumed mass at saturation from the thin film results. Mathematical and finite element models to predict the transverse diffusivity of a unidirectional composite based on the diffusivity of the matrix did not capture the observed trends. Given the disparity between experimental and modelling results, it appears that experimental studies of a given epoxy and carbon/epoxy composite are required to predict the nature of diffusion in an epoxy and the transverse diffusivity of the composite.

Data Availability

The data that support the findings of this study are available from the corresponding author upon reasonable request.

Conflicts of Interest

The authors declare that there is no conflict of interest regarding the publication of this paper.

Acknowledgments

The authors are very grateful to SACAC Ltd, Dr. Giovanni Terrasi from EMPA, and Dr. Michael Sutcliffe from the University of Cambridge for their support and guidance. The first author was funded through an EPSRC doctoral training award (EP/P500117/1).

Supplementary Materials

The supplementary material "experimental details of transverse diffusivity studies" includes the transverse diffusivity values, fibre content, and exposure conditions of all transverse diffusivity studies in CFRPs used in Figures 3, 6, and 7 and Table 1, as found in literature. Supporting information is available from the Wiley Online Library. *(Supplementary Materials)*

References

[1] M. S. Dresselhaus, G. Dresselhaus, K. Sugihara, I. L. Spain, and H. A. Goldberg, *Graphite Fibres and Filaments*, Springer-Verlag, Berlin Heidelberg, Berlin, 1988.

[2] Z. R. Yue, W. Jiang, L. Wang, S. D. Gardner, and C. U. Pittman, "Surface characterization of electrochemically oxidized carbon fibers," *Carbon*, vol. 37, no. 11, pp. 1785–1796, 1999.

[3] J. B. Donnet and R. C. Bansal, *Carbon Fibres*, Marcel Dekker, New York, 1990.

[4] I. M. K. Ismail, "On the reactivity, structure, and porosity of carbon fibers and fabrics," *Carbon*, vol. 29, no. 6, pp. 777–792, 1991.

[5] K. Kondo and T. Taki, *Moisture Diffusivity of Unidirectional Composites, in Environmental Effects on Composite Materials*, Technomic Publishing Co., Lancaster, PA, USA, 1984.

[6] N. C. W. Judd, "Absorption of water into carbon fibre composites," *British Polymer Journa*, vol. 9, no. 1, pp. 36–40, 1977.

[7] M. Blikstad, "Three-dimensional moisture diffusion in graphite/epoxy laminates," *Journal of Reinforced Plastics and Composites*, vol. 5, no. 1, pp. 9–18, 1986.

[8] J. P. Soulier, R. Berruet, A. Chateauminois, R. Chabert, and R. Gauthier, "Interactions of fibre-reinforced epoxy composites with different salt water solutions," *Polymer communications (Guildford)*, vol. 29, no. 8, pp. 243–246, 1988.

[9] C. H. Shen and G. S. Springer, "Moisture absorption and desorption of composite materials," *Journal of Composite Materials*, vol. 10, no. 1, pp. 2–20, 1976.

[10] D. A. Bond, "Moisture diffusion in a fiber-reinforced composite: part I – non-Fickian transport and the effect of fiber spatial distribution," *Journal of Composite Materials*, vol. 39, no. 23, pp. 2113–2141, 2005.

[11] A. B. Strong, *Plastics: Materials and Processing*, Pearson Prentice Hall, Upper Saddle River, NJ, 2000.

[12] R. Martin and R. Campion, "The effects of aging on fibre reinforced plastics," *Materials World*, vol. 4, p. 200, 1981.

[13] M. R. Vanlandingham, R. F. Eduljee, and J. W. Gillespie, "Moisture diffusion in epoxy systems," *Journal of Applied Polymer Science*, vol. 71, no. 5, pp. 787–798, 1999.

[14] J. Zhou and J. P. Lucas, "Hygrothermal effects of epoxy resin. Part I: the nature of water in epoxy," *Polymer*, vol. 40, no. 20, pp. 5505–5512, 1999.

[15] Y. Diamant, G. Marom, and L. J. Broutman, "The effect of network structure on moisture absorption of epoxy resins," *Journal of Applied Polymer Science*, vol. 26, no. 9, pp. 3015–3025, 1981.

[16] M. J. Adamson, "Thermal expansion and swelling of cured epoxy resin used in graphite/epoxy composite materials," *Journal of Materials Science*, vol. 15, no. 7, pp. 1736–1745, 1980.

[17] J. E. Sumerak and J. D. Martin, *Pultrusion in Engineered Materials Handbook Desk Edition*, M. G. Gauthier, Ed., ASM international, 1995.

[18] R. Sen, M. Shahawy, S. Sukumar, and J. Rosas, "Durability of carbon pretensioned elements in a marine environment," *Structural Journal*, vol. 95, no. 6, pp. 716–724, 1998.

[19] W. M. Cross, F. Johnson, J. Mathison, C. Griswold, J. J. Kellar, and L. Kjerengtroen, "The effect of interphase curing on interphase properties and formation," *The Journal of Adhesion*, vol. 78, no. 7, pp. 571–590, 2002.

[20] Y. Joliff, W. Rekik, L. Belec, and J. F. Chalian, "Study of the moisture/stress effects on glass fibre/epoxy composite and the impact of the interphase area," *Composite Structures*, vol. 108, pp. 876–885, 2014.

[21] J. D. H. Hughes, "The carbon fibre/epoxy interface—a review," *Composites Science and Technology*, vol. 41, no. 1, pp. 13–45, 1991.

[22] R. D. Adams and M. M. Singh, "The dynamic properties of fibre-reinforced polymers exposed to hot, wet conditions," *Composites Science and Technology*, vol. 56, no. 8, pp. 977–997, 1996.

[23] F. A. Ramirez, L. A. Carlsson, and B. A. Acha, "Evaluation of water degradation of vinylester and epoxy matrix composites by single fiber and composite tests," *Journal of Materials Science*, vol. 43, no. 15, pp. 5230–5242, 2008.

[24] Z. Wang, G. Xian, and X. L. Zhao, "Effects of hydrothermal aging on carbon fibre/epoxy composites with different interfacial bonding strength," *Construction and Building Materials*, vol. 161, pp. 634–648, 2018.

[25] A. Gagani, A. Krauklis, and A. T. Echtermeyer, "Anisotropic fluid diffusion in carbon fiber reinforced composite rods: experimental, analytical and numerical study," *Marine Structures*, vol. 59, pp. 47–59, 2018.

[26] V. M. Karbhari and G. Xian, "Hygrothermal effects on high VF pultruded unidirectional carbon/epoxy composites: moisture uptake," *Composites Part B: Engineering*, vol. 40, no. 1, pp. 41–49, 2009.

[27] J. Crank, *The Mathematics of Diffusion*, Oxford University Press, London, UK, 1975.

[28] P. Scott and J. M. Lees, "Water, salt water, and alkaline solution uptake in epoxy thin films," *Journal of Applied Polymer Science*, vol. 130, pp. 1898–1908, 2013.

[29] T. I. Glaskova, R. M. Guedes, J. J. Morais, and A. N. Aniskevich, "A comparative analysis of moisture transport models as applied to an epoxy binder," *Mechanics of Composite Materials*, vol. 43, no. 4, pp. 377–388, 2007.

[30] W. K. Loh, A. D. Crocombe, M. M. Abdel Wahab, and I. A. Ashcroft, "Modelling anomalous moisture uptake, swelling and thermal characteristics of a rubber toughened epoxy adhesive," *International Journal of Adhesion and Adhesives*, vol. 25, no. 1, pp. 1–12, 2007.

[31] P. Scott, *Aspects of CFRP prestressed concrete durability in the marine environmnent, [Ph.D. thesis]*, University of Cambridge, 2009.

[32] K. Kondo and T. Taki, "Moisture diffusivity of unidirectional composites," *Journal of Composite Materials*, vol. 16, no. 2, pp. 82–93, 1982.

[33] B. Dewimille and A. R. Bunsell, "The modelling of hydrothermal aging in glass fibre reinforced epoxy composites," *Journal of Physics D: Applied Physics*, vol. 15, no. 10, pp. 2079–2091, 1982.

[34] H. B. Keller and D. Sachs, "Calculations of the conductivity of a medium containing cylindrical inclusions," *Journal of Applied Physics*, vol. 35, no. 3, pp. 537-538, 1964.

[35] W. L. Ko, "Transverse diffusivity of dual phase composites," *Fibre Science and Technology*, vol. 11, no. 2, pp. 157–162, 1978.

[36] M. A. Abanilla, Y. Li, and V. M. Karbhari, "An experimental, analytical and numerical study of the static behavior of steel beams reinforced by pultruded CFRP strips," *Composites Part B: Engineering*, vol. 37, no. 1, pp. 64–73, 2006.

[37] R. E. Bohlman and E. A. Derby, "Moisture Diffuion in Graphite/Epoxy Laminates: Experimental and Presicted," in *AIAA/ASME 18th Structural Dynamics & Materials Conference*, vol. A, pp. 219–226, San Diego, 1977.

[38] R. Delasi and J. B. Whiteside, *Advanced Composite Materials—Environmental Effects*, J. Vinson, Ed., ASTM International, West Conshohocken, PA, 1978.

[39] B. Hong, G. Xian, and Z. Wang, "Durability study of pultruded carbon fiber reinforced polymer plates subjected to water immersion," *Advances in Structural Engineering*, vol. 21, no. 4, pp. 571–579, 2018.

[40] J. C. Arnold, S. M. Alston, and F. Korkees, "An assessment of methods to determine the directional moisture diffusion coefficients of composite materials," *Composites Part A: Applied Science and Manufacturing*, vol. 55, pp. 120–128, 2013.

[41] F. Korkees, S. Alston, and C. Arnold, "Directional diffusion of moisture into unidirectional carbon fiber/epoxy composites: experiments and modeling," *Polymer Composites*, vol. 39, no. S4, pp. E2305–E2315, 2018.

[42] J. W. Chin, T. Nguyen, and K. Aouadi, "Sorption and diffusion of water, salt water, and concrete pore solution in composite matrices," *Journal of Applied Polymer Science*, vol. 71, no. 3, pp. 483–492, 1999.

[43] M. Blikstad, P. O. W. Sjoblom, and T. R. Johannesson, "Long-term moisture absorption in graphite/epoxy angle-ply laminates," *Journal of Composite Materials*, vol. 18, no. 1, pp. 32–46, 1984.

[44] D. W. Suh, M. K. Ku, J. D. Nam, B. S. Kim, and S. C. Yoon, "Equilibrium water uptake of epoxy/carbon fiber composites in hygrothermal environmental conditions," *Journal of Composite Materials*, vol. 35, no. 3, pp. 264–278, 2001.

[45] H. G. Carter and K. G. Kibler, "Langmuir-type model for anomalous moisture diffusion in composite resins," *Journal of Composite Materials*, vol. 12, no. 2, pp. 118–131, 1978.

[46] I. B. C. M. Rocha, S. Raijmaekers, F. P. van der Meer, and L. J. Sluys, "Combined experimental/numerical investigation of directional moisture diffusion in glass/epoxy composites," *Composites Science and Technology*, vol. 151, pp. 16–24, 2017.

[47] ASTM D823, *Standard Practices for Producing Films of Uniform Thickness of Paint, Varnish, and Related Products on Test Panels*, ASTM International, West Conshohocken, PA, 2017.

[48] ASTM D5229/D5229M-20, *Standard Test Method for Moisture Absorption Properties and Equilibrium Conditioning of Polymer Matrix Composite Materials*, ASTM International, West Conshohocken, PA, 2020.

[49] E. Toumpanaki, J. M. Lees, M. Barbezat, and G. P. Terrasi, "Effect of internal moisture content and dynamic mechanical analysis testing conditions on the T values of CFRP tendons," *Construction and Building Materials*, vol. 227, article 116771, 2019.

[50] MATLAB, *MATLAB*, The MathWorks, Natick, MA, USA, 2019.

[51] E. Toumpanaki, J. M. Lees, and G. P. Terrasi, "Bond durability of carbon fiber–reinforced polymer tendons embedded in high-strength concrete," *Journal of Composites for Construction*, vol. 22, no. 5, article 04018032, 2018.